GEOLOGY OF THE INTERMOUNTAIN WEST
an open-access journal of the Utah Geological Association
ISSN 2380-7601
Volume 9 *2022*

GEOMORPHIC AND TECTONIC DEVELOPMENT OF SWAN VALLEY, SOUTHEAST IDAHO, SINCE THE ERUPTION OF THE BASALT OF ANTELOPE FLAT—NEW ^{40}AR/^{39}AR, GEOCHEMICAL, AND PALEOMAGNETIC DATA

Stacy Henderson, Tiffany Rivera, Peter C. Lippert, and Brian R. Jicha

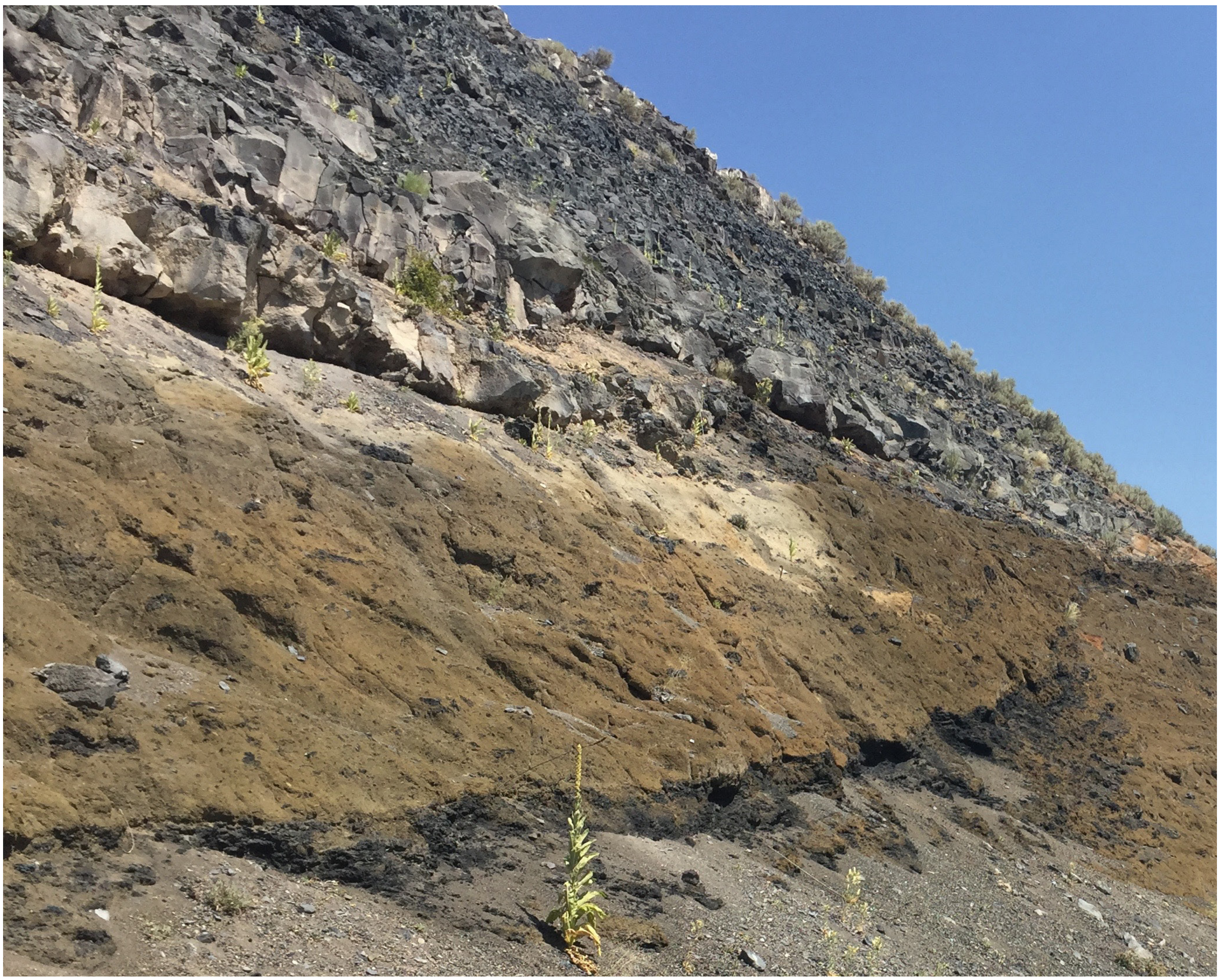

GEOLOGY OF THE INTERMOUNTAIN WEST

an open-access journal of the Utah Geological Association

ISSN 2380-7601

Volume 9 **2022**

Cover

The Pleistocene Basalt of Antelope Flat dammed the Snake River in Swan Valley, southeast Idaho, producing hyaloclastite visible along US Highway 26.

Become a member of the UGA to help support the work of the Association and receive notices for monthly meetings, annual field conferences, and new publications. Annual membership is $20 and annual student membership is only $5. Visit the UGA website at www.utahgeology.org for information and membership application.

The UGA board is elected annually by a voting process through UGA members. However, the UGA is a volunteer-driven organization, and we welcome your voluntary service. If you would like to participate please contact the current president or committee member corresponding with the area in which you would like to volunteer.

Utah Geological Association formed in 1970 from a merger of the Utah Geological Society, founded in 1946, and the Intermountain Association of Geologists, founded in 1949. Affiliated with the American Association of Petroleum Geologists.

GEOLOGY OF THE INTERMOUNTAIN WEST
an open-access journal of the Utah Geological Association
Volume 9 *2022*

Geomorphic and Tectonic Development of Swan Valley, Southeast Idaho, Since the Eruption of the Basalt of Antelope Flat—New $^{40}Ar/^{39}Ar$, Geochemical, and Paleomagnetic Data

Stacy Henderson[1, 2], Tiffany Rivera[1], Peter C. Lippert[3], and Brian R. Jicha[4]
[1] Westminster College, 1840 South 1300 East, Salt Lake City, UT 84105; trivera@westminstercollege.edu
[2] Montana State University, Culbertson Hall, 100, Bozeman, MT 59717; stacy.henderson@student.montana.edu
[3] Department of Geology and Geophysics, University of Utah, 115 S 1460 E, Salt Lake City, UT 84112; pete.lippert@utah.edu
[4] Department of Geoscience, University of Wisconsin-Madison, 1215 West Dayton Street, Madison, WI 53706; brian.jicha@wisc.edu

ABSTRACT

Swan Valley is a graben in eastern Idaho that formed by extension along the Grand Valley and Snake River faults and preserves a record of explosive rhyolitic volcanism sourced from the Yellowstone Plateau and Heise volcanic fields, as well as locally sourced basaltic lavas. The Pleistocene Basalt of Antelope Flat intersected the South Fork of the Snake River and generated a temporary hyaloclastite dam. Previous workers proposed that the lava dam allowed for the accumulation of water that led to the generation of paleo-Swan Lake. Although lacustrine deposits from paleo-Swan Lake have not been described or mapped, several-meters thick intercalated hyaloclastites and pillow lavas require the interaction between continued volcanism and standing water. In this work, we present new geochemical, geochronologic, and paleomagnetic data to reinterpret the eruptive history of the basalts within the valley, estimate the volume and duration to fill paleo-Swan Lake, and calculate incision rates of the Snake River through Quaternary basalts. Using geochemical and paleomagnetic data, we reinterpret deposits previously mapped as the Basalt of Antelope Flat as three temporally distinct units. The duration to fill paleo-Swan Lake is calculated as 12 to 20 years. An absence of lacustrine deposits, shorelines, or other indicators of a lake environment led us to propose that shallow, marshy, wetland conditions existed locally to produce hydrovolcanic deposits characteristic of the Basalt of Antelope Flat. We report a new $^{40}Ar/^{39}Ar$ age of 904 ± 11 ka (2σ) for the Basalt of Antelope Flat, which we use to determine an average incision rate of 0.014 cm/yr for the Snake River through Quaternary basalts. Our multi-method approach provides updated constraints to the eruptive and geomorphological history of southeastern Idaho.

INTRODUCTION

The Snake River Plain-Yellowstone (SRP-Y) volcanic province is known for its time-transgressive caldera-forming super-eruptions, numerous inter- and intra-caldera rhyolite domes, and voluminous basaltic lava flows that bury most older calderas (Christiansen, 2001). SRP-Y volcanic activity for the past 16 million years spans southern Idaho and northwestern Wyoming. Volcanism and related tectonism are often attributed to the passage of North America over a stationary hotspot (Pierce and Morgan, 1992; Smith and

Citation for this article.
Henderson, S., Rivera, T., Lippert, P.C., and Jicha, B.R., 2022, Geomorphic and tectonic development of Swan Valley, southeast Idaho, since the eruption of the Basalt of Antelope Flat—new $^{40}Ar/^{39}Ar$, geochemical, and paleomagnetic data: Geology of the Intermountain West, v. 9, p. 115–130, https://doi.org/10.31711/giw.v9.pp115-130.

Braile, 1994; Camp, 1995), although small-scale upper mantle convection (Humphreys and others, 2000) or mantle return flow around the subducting Farallon slab remnant (James and others, 2011; Fouch, 2012) have also been proposed.

The rhyolitic products of the SRP-Y province have been intensely studied for their distribution, geochemistry (Hamilton, 1965; Christiansen and Blank, 1972; Christiansen, 1982, 2001), geochronology (e.g., Obradovich, 1992; Rivera and others, 2017), super-eruption cycles (Christiansen and Blank, 1972; Christiansen, 1982, 2001; Obradovich, 1992; Rivera and others, 2017), and rates of magmatic evolution (Rivera and others, 2014, 2016, 2017; Matthews and others, 2015; Stelten and others, 2015; Troch and others, 2017; Shamloo and Till, 2019, 2021). Basaltic eruptions across the SRP-Y province have provided myriad insights into physical and chemical processes associated with lithospheric structure (e.g., Shervais and Hanan, 2008), melt generation and differentiation (e.g., Leeman, 1976; Hughes and others, 2002; Putrika and others, 2009; Rivera and others, 2021), and eruption characteristics (e.g., Greeley, 1982; Kunz, 1982; Creighton, 1987).

The interaction of Pleistocene basaltic lavas with water is preserved in areas of the Snake River Plain. Lavas have filled paleo-channels and dammed and diverted rivers, and rivers and flooding have incised deep canyons through these basalts. For example, the South Fork of the Boise River was dammed multiple times over a 2-million-year period (Howard and others, 1982) and basalts erupted from McKinney Butte dammed the Snake River near Bliss, Idaho, generating a lava delta with abundant pillow basalts (Malde, 1971,1982). At American Falls, the 70 ka Cedar Butte lava flow dammed the Snake River; the lava dam led to the filling of American Falls Lake, which persisted until the Bonneville Flood (Scott and others, 1982). The Snake River Canyon and the Malad Gorge, both in the central Snake River Plain, are two examples of incised canyons that were carved by the downcutting of rivers (Lamb and others, 2014).

Swan Valley is a graben in eastern Idaho that formed by extension along the Grand Valley and Snake River faults. The graben preserves a record of both explosive and effusive volcanism from the Yellowstone Plateau (0 to 2 Ma) and Heise (4.5 to 6.6 Ma) volcanic fields (figure 1), as well as locally sourced basaltic lavas. One of these local effusive eruptions is the Basalt of Antelope Flat. Originally described by Hackett and Morgan (1988) as part of the Conant Valley volcanics, Dossett and others (2012) later divided the deposit into multiple facies including rim and canyon-filling subaerial facies, a dam complex facies, and a hyaloclastite facies. These observations led previous workers to propose that the Basalt of Antelope Flat dammed the channelized Snake River and impounded water upstream, producing a short-lived lake (Hackett and Morgan, 1988; Moore and Embree, 2016). Continued eruption of basalt allowed for the development of pillow lavas as flows entered the shallow standing water upstream and fluvial deposition continued downstream of the lava dam. Termed Swan Lake (Moore and Embree, 2016), this impoundment persisted for some unknown time until the dam was breached, causing the Snake River to divert its course and join a second drainage, which now forms the present-day canyon. Swan Lake is hypothesized to extend nearly 50 km toward the southeast and occupy an area twice the size of the present-day Palisades Reservoir (Moore and Embree, 2016).

In this contribution, we present a new $^{40}Ar/^{39}Ar$ eruption age, as well as geochemistry and paleomagnetic data for the Basalt of Antelope Flat. With these data, we reinterpret the Quaternary geology of Swan Valley to (1) assess the eruptive history of basalts within the valley, (2) estimate the volume and fill rate for Swan Lake, and (3) calculate incision rates of the diverted Snake River through Quaternary basalts.

MATERIALS AND METHODS

Planar- and cross-bedded hyaloclastite consists of juvenile sand-size, angular, dark brown glassy basalt fragments, with a weathered, burnt orange palagonitic cement. Accidental clasts include quartz arenite, vesicular basalt, and dense rhyolite cobbles and pebbles (Hackett and Morgan, 1988). Approximately 80 m of subaerial lavas, basal tuff breccias interpreted as mass wasting deposits from failure of water-saturated palagonite tuffs, cross-bedded laminated tuffs interpreted as

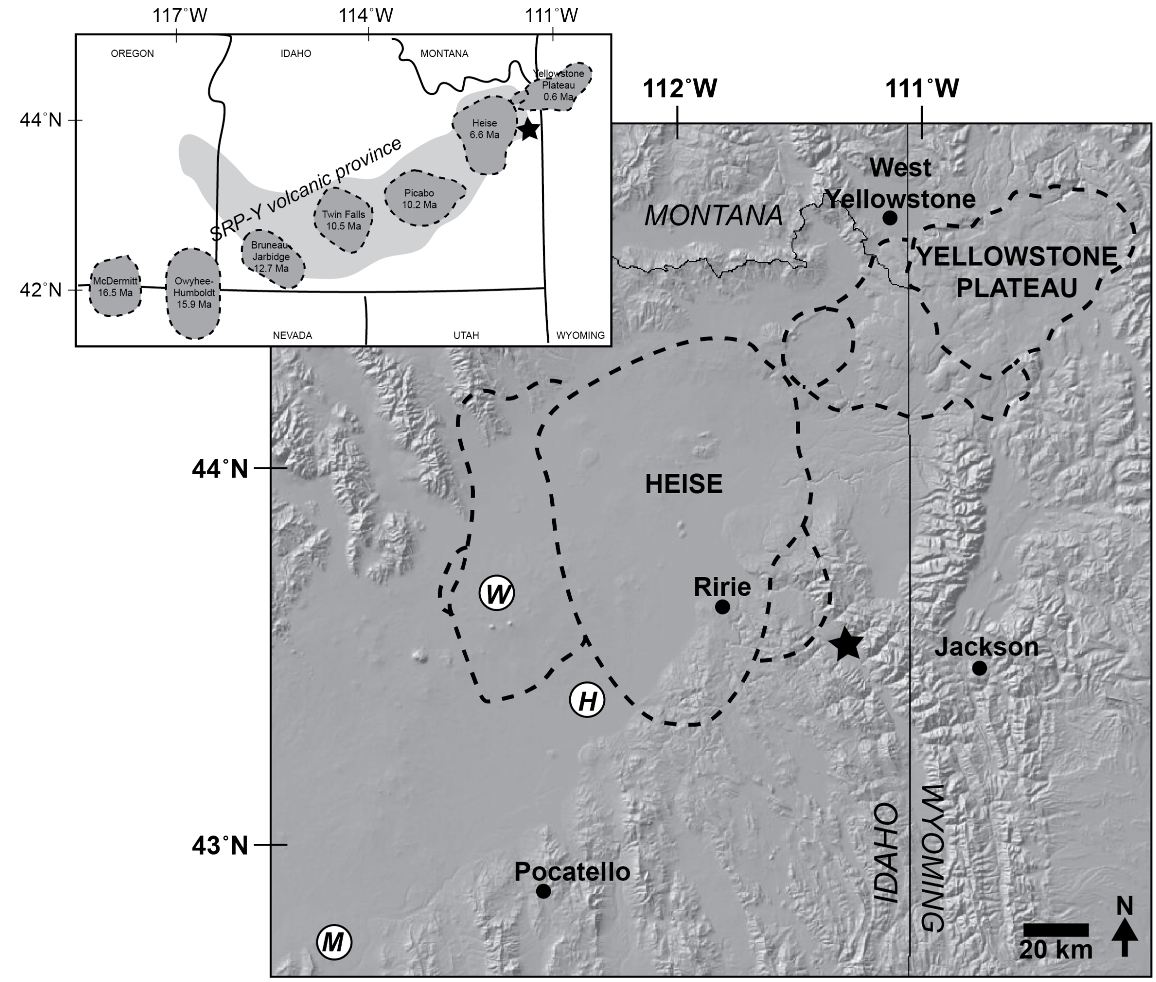

Figure 1. Location map of the Heise and Yellowstone volcanic fields in the eastern Snake River Plain (SRP), Idaho and northwestern Wyoming. Caldera boundaries are indicated by the dashed lines. Swan Valley is indicated by the star (detail is provided in figure 2). Inset map shows the calderas of the SRP resulting from hotspot-related volcanism. Base map generated from GeoMapApp; map modified from Bindeman and others (2007) and Watts and others (2011). Approximate locations (not to scale) of basaltic lavas discussed in text are denoted by M (Massacre Rocks State Park), H (Hell's Half Acre), and W (Idaho National Laboratory drill core WO-2).

lacustrine deposits, and subaerial flows with pillow bases indicative of flow into shallow standing water, are present within the Swan Valley graben (Hackett and Morgan, 1988; Dossett and others, 2012; Moore and Embree, 2016). Poor sorting and the absence of bomb sags were interpreted as evidence for deposition as a sheet wash, rather than indicating proximal air-fall deposits (Hackett and Morgan, 1988). For this work, we sampled the Basalt of Antelope Flat dam complex and hyaloclastite facies (location 1 in figure 2). The dam complex lava (samples 16AF-1 and 17AF-2) is a dark gray, vesicular basalt (figure 3) with phenocrysts of olivine and plagioclase and minimal secondary mineralization in the vesicles (figure 4). The hyaloclastite sample (17AF-3) consists of glassy brown to black sand-size basaltic fragments.

Paleomagnetic Methods

Eleven 2.5-cm-diameter cores approximately 10 to 15 cm in length were drilled from a single flow in the dam facies of the Basalt of Antelope Flat (sample 17AF-2) on the northeast side of State Highway 26 in Idaho (43.4891° N, 111.4494° W). Cores were drilled using a gasoline-powered drill over 1 vertical m and several lateral meters of outcrop. Cores were oriented in situ using a magnetic compass. The cores were cut into 10 cm^3 specimens and the freshest specimens from each sample were used for analysis at the Utah Paleomagnetic Center at the University of Utah. The natural remanent magnetism (NRM) of each 10 cm^3 core specimen was measured using an AGICO JR6A spinner magnetometer operating in the fast, six-position automatic mode. The NRM was demagnetized along the x, y, and z axes using alternating fields in steps from 5 mT to 300 mT (as required by specimen) with a minimum of 14 steps using a Magnon 300 Alternating Field Demagnetizer. Measurement was stopped when the specimens retained <10% of their original magnetic intensity.

^{40}Ar/^{39}Ar Dating Methods

Bulk rock of the Basalt of Antelope Flat (sample 16AF-1) was crushed, milled, and sieved to the 180 to 250 µm fraction at the University of Wisconsin-Madison. This fraction was purified using a combination of magnetic separation and handpicking to ensure a phenocryst-free groundmass. Groundmass was irradiated for three hours with the Alder Creek Rhyolite sanidine

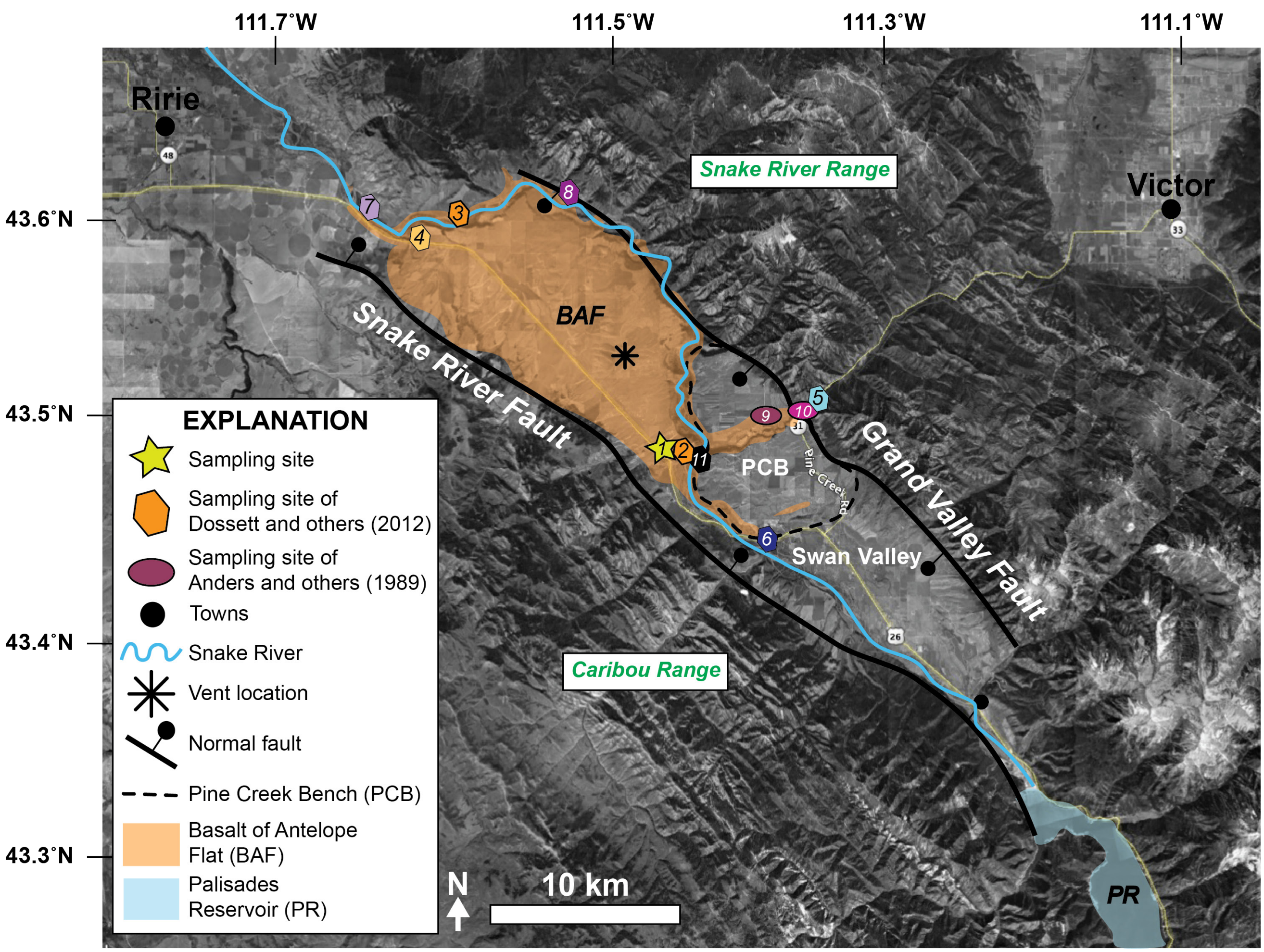

Figure 2. Location of Swan Valley and sampling sites of the Basalt of Antelope Flat and other lavas discussed in this text. Lava flow, coordinates, and other data are provided in table 2. The star symbol is the sampling location for original data presented here; ovals are sampling locations of Anders and others (1989); hexagons are sampling locations of Dossett and others (2012). Pine Creek Bench (PCB) is the area enclosed by the broken line. The downthrown sides of the Snake River and Grand Valley faults are indicated by the ball and stick. Fault locations, vent, and distribution of the Basalt of Antelope Flat are approximate. Extent of the basalt is interpreted from the geologic map, cross sections, and well logs of Dossett and others (2012). Base map generated from Google Earth.

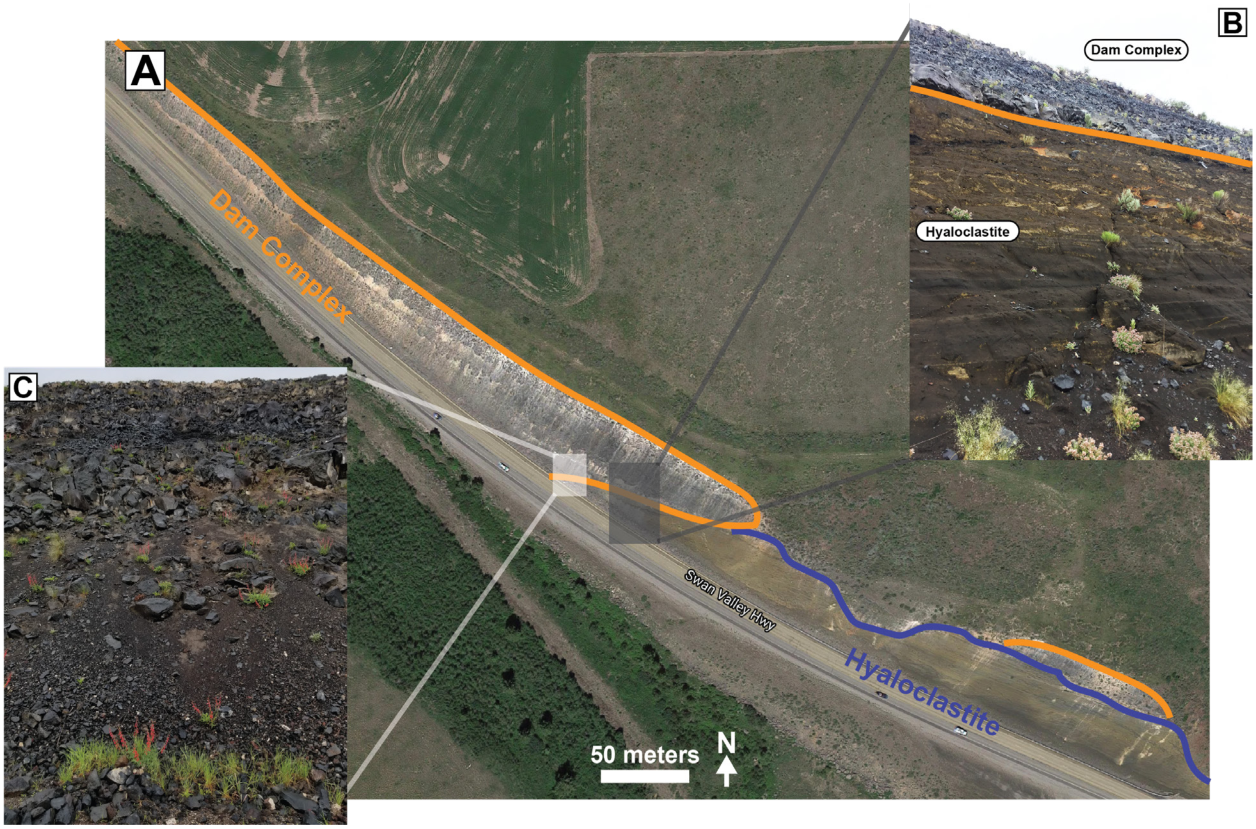

Figure 3. Outcrop of the Basalt of Antelope Flat (location 1 on figure 2). (A) Google Earth image of the road cut with the dam complex and hyaloclastite facies indicated. (B) Palagonitic to glassy hyaloclastite capped by the dam complex facies. (C) Dark gray to black vesicular Basalt of Antelope Flat dam complex facies.

standard at Oregon State University in the Cadmium-Lined in-Core Irradiation Tube (CLICIT) facility. Upon return, argon isotopic analyses were conducted using a 60W CO_2 laser and a Nu Instruments Noblesse multi-collector mass spectrometer following the procedures of Jicha and others (2016). Analyses of the Alder Creek Rhyolite sanidine were conducted as single crystal fusion experiments, whereas the groundmass of the Basalt of Antelope Flat was analyzed by incremental heating. Ages are reported relative to an Alder Creek Rhyolite sanidine standard age of 1.1864 Ma (Rivera and others, 2013; Jicha and others, 2016) and decay constants of Min and others (2000). Uncertainties are reported at 2σ and include the error contribution from the irradiation parameter *J*, unless otherwise indicated.

Geochemistry Methods

Geochemical analyses were performed on dense, fresh, crushed whole rock powder made from the dam complex facies sample 17AF-2, whereas hand-picked glassy fragments of the hyaloclastite were used for analysis of sample 17AF-3. All analyses were conducted at the Peter Hooper GeoAnalytical Lab at Washington State University. Major and minor element analyses were conducted by X-ray fluorescence (XRF) whereas trace and rare earth elements were conducted by inductively coupled plasma mass spectrometry (ICPMS).

RESULTS

Paleomagnetic Results

All 11 Basalt of Antelope Flat core specimens exhibited similar demagnetization behavior. A consistent and well-defined characteristic remanent magnetization (ChRM) is evident after a steep downward direction was removed between 5 and 10 mT; the ChRM is southwest and up and decays toward the origin of orthogonal vector plots (table 1; appendix). We interpret the low coercivity downward component as a recent magnetic overprint and the ChRM as the primary magnetization acquired at the time of eruption. Directions from 8 of the 11 specimens were used to determine the site mean direction. Three specimens were excluded due to outlying declination directions (figure 5). The remaining eight specimens cluster tightly and clearly indicate a reverse polarity ChRM direction fit by principal component analysis (PCA; Kirschvink, 1980). The Fisher mean direction is an inclination of -36.5° and a declination of 247.3° (α_{95} = 3.3°, κ = 287.6; figure 5, table 1). The site mean direction differs from the time-averaged dipole direction at this site, but this can be explained by secular variation of the geomagnetic field at the time of eruption. Importantly, a single lava flow is not expected to record a time-averaged direction. The magnetic polarity recorded by the Basalt of Antelope Flat is unambiguously reversed.

$^{40}Ar/^{39}Ar$ Dating Results

Two incremental heating experiments of groundmass from the Basalt of Antelope Flat (sample 16AF-1) produced plateaus with >75% of the $^{39}Ar_K$ released. Plateau-defining steps are presented in blue (figure 6); steps excluded from the plateau age are presented in white. Plateaus were achieved with 9 out of 12 heating steps in the first analysis and 5 out of 11 heating steps in the second analysis. The first experiment yielded a plateau age of 893 ± 18 ka (2σ, including *J*; figure 6A). The second experiment yielded a plateau age of 910 ± 14 ka (2σ, including *J*; figure 6B). Combining the ages of the two experiments yields a weighted mean age of 904 ± 11 ka (2σ, including *J*). Full analytical data are provided in the appendix.

Geochemical Results

The Basalt of Antelope Flat has a SiO_2 content of about 48 weight percent (wt.%) and total alkali content ($Na_2O + K_2O$) of about 3 wt.%, thus placing the sample within the field of "basalt" on a total alkali versus silica diagram (Le Bas and others, 1986). Figure 7 shows major element oxides and selected trace element concentrations (parts per million [ppm]) for the Basalt of Antelope Flat dam and hyaloclastite facies in comparison to several other basalts of the eastern Snake River Plain (ESRP) region. The hyaloclastite glass has slightly

Table 1. Site 17AF2 – Antelope Flats (43.489239°N, 111.449723°W). Demagnetization steps, mean angular deviation (MAD) of the Characteristic Remanent Magnetization (ChRM) fit, declination (Dg), and inclination (Ig) of 11 analyses of the Basalt of Antelope Flat. N: number of consecutive demagnetization steps used to define the ChRM.

Specimen Number	Demagnetization Steps	N	MAD	Ig	Dg
17AF2.1	40-150 mT	7	2.8	-26.9	229.0
17AF2.2	40-175 mT	8	2.9	-35.0	246.9
17AF2.3	80-275 mT	9	8.9	-33.4	250.6
17AF2.4	40-250 mT	10	3.6	-37.9	254.4
17AF2.5	40-250 mT	10	3.2	-34.5	244.6
17AF2.6	50-200 mT	8	4.7	-40.3	243.9
17AF2.7	50-200 mT	8	4.1	-36.8	243.3
17AF2.8	80-175 mT	5	8.9	-37.0	254.5
17AF2.9	50-225 mT	9	3.1	-36.6	240.2
17AF2.10	50-225 mT	9	4.1	-35.6	271.4
17AF2.11	50-175 mT	7	4.0	-31.2	267.5

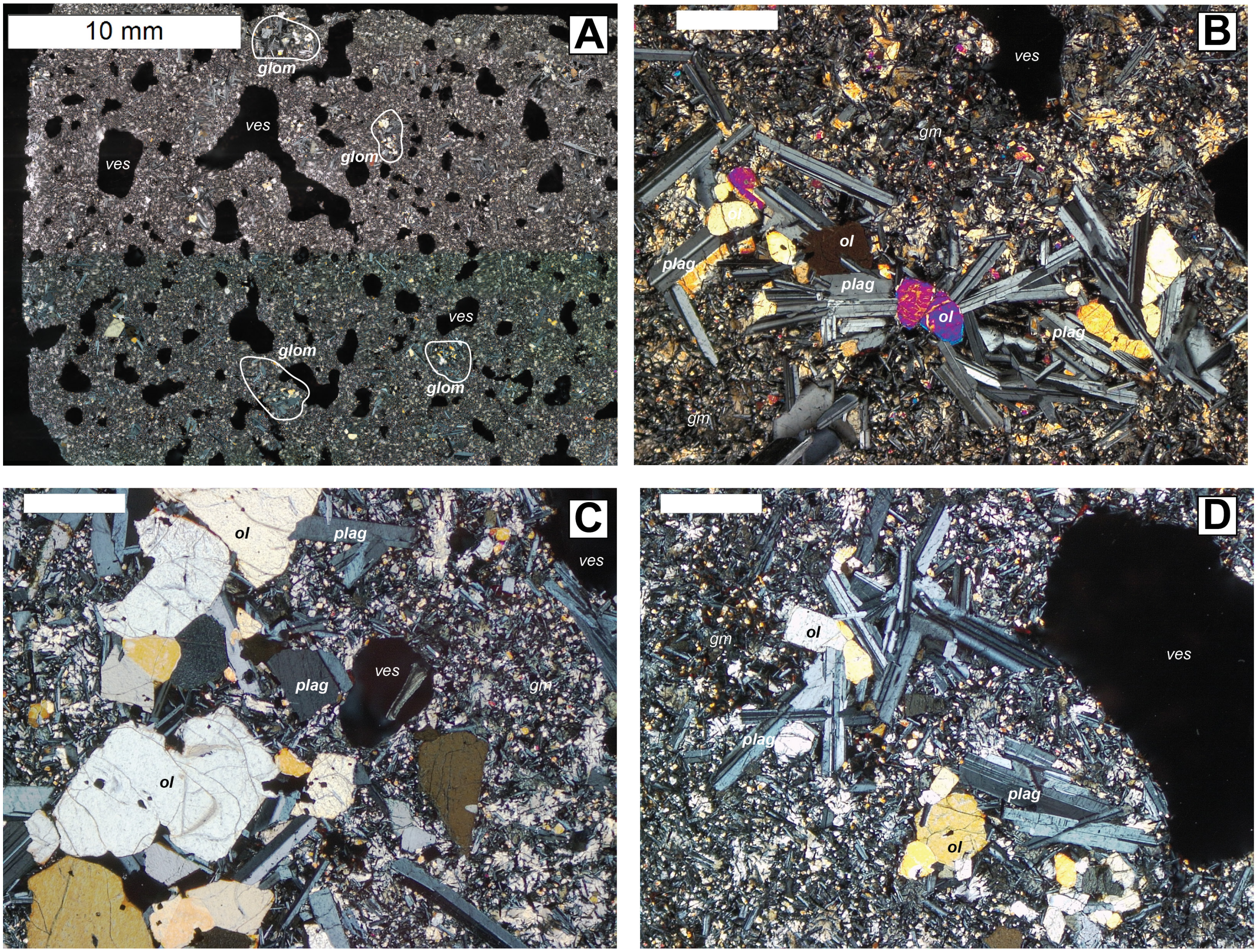

Figure 4. Basalt of Antelope Flat dam complex facies (sample 17AF-2) in thin section. All images are in cross-polarized light. (A) Vesicular basalt. (B, C, D) Glomerocrysts of olivine and plagioclase laths set in a fine-grained groundmass. Scale bar in B, C, and D is 500 micrometers; ves: vesicle, glom: glomerocryst, ol: olivine, plag: plagioclase, gm: groundmass.

lower SiO_2, Al_2O_3, CaO, and total alkali relative to the dam facies. It also had a higher volatile concentration as measured by "loss on ignition," which may be due to the inclusion of some hydrated palagonitic glass in the sample during handpicking. Full analytical data are provided in the appendix.

DISCUSSION

Geochemistry

We compare the composition of our sample of the Basalt of Antelope Flat to several suites of Snake River Plain basalts (figures 1 and 7). The Idaho National Lab (INL) WO-2 drill core sampled basalt lavas at depth with ages that range from about 0.2 to about 2.3 Ma (Shervais and others, 1994). Hell's Half Acre is located within the ESRP, and is geographically closer to Swan Valley, but the lavas are substantially younger than the Basalt of Antelope Flat (^{14}C age of 5200 ± 150 years before present as of Kuntz and others, 1986). The 6.3 Ma (Armstrong and others, 1975) basalts of the Massacre Volcanics erupted along the southern margin of the

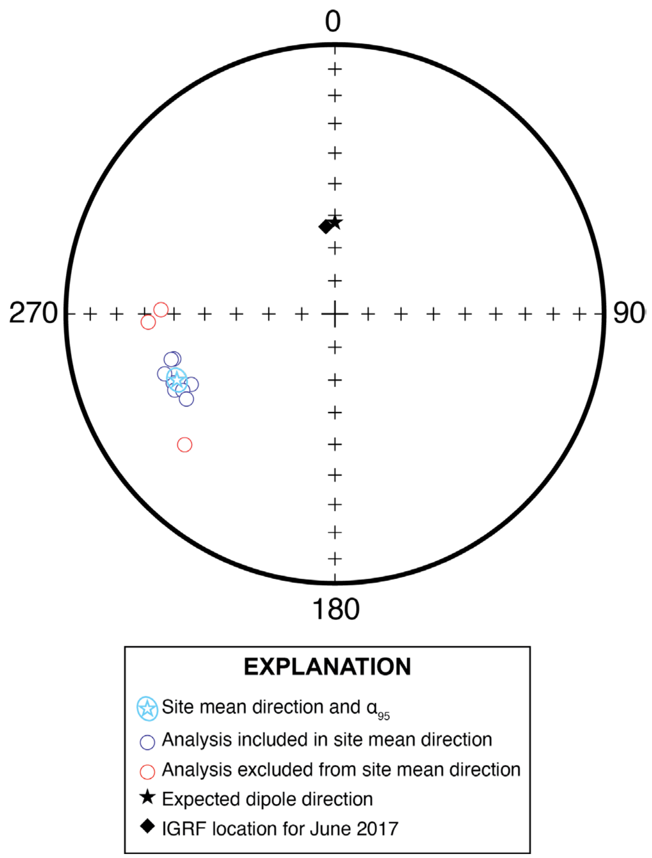

Figure 5. Stereonet of site mean direction, expected dipole direction, and the International Geomagnetic Reference Field (IGRF) direction for June 2017 when sample 17AF-2 was obtained.

fault-bounded ESRP. Our samples are geochemically most similar to the temporally equivalent lavas encountered at depth within the INL core (figure 7). Although SRP lavas are notorious for their elevated P_2O_5 contents (e.g., Leeman, 1982), as demonstrated in the young lavas at Hell's Half Acre, the Basalt of Antelope Flat does not show the elevated P_2O_5 at similar SiO_2 contents. Furthermore, the Basalt of Antelope Flat has elevated TiO_2, Sr, and Zr but lower MgO relative to the basalts of the Massacre Volcanics, thus making them dissimilar to this older suite of basaltic lavas. These geochemical variations may signify derivation from different mantle source regions or may be indicative of processes such as fractional crystallization or assimilation of country rock occurring at shallow depths prior to eruption. The petrogenetic processes governing the chemical variability are beyond the scope of this work.

Basalt Flows of the Swan Valley Graben

The Swan Valley graben has three prominent areas where basaltic lavas are present (figures 2 and 8; Dossett and others, 2012). The northwesternmost area is Antelope Flat, which is dominated by the Basalt of Antelope Flat and is bound by the Snake River on its eastern side. At a similar elevation, Pine Creek Bench is dissected by the Snake River on the west and by Pine Creek across the center of the bench. Here, the 4.0 Ma Basalt of Swan Valley and a paleocanyon-filling facies of the Basalt of Antelope Flat are exposed near the mouth of Pine Creek Canyon, where Pine Creek joins the Snake River (Anders and others, 1989; Dossett and others, 2012). The paleocanyon facies may contain three to five different flow units (Dossett and others, 2012). The dam, rim, and hyaloclastite facies of the Basalt of Antelope Flat are prominent at the confluence between Pine Creek Bench and Antelope Flat. The rim facies is characterized by columnar jointing and pillow bases. The 4.0-Ma Basalt of Swan Valley is also exposed here (Dossett and others, 2012). Swan Valley is the topographically lower area to the southeast of Pine Creek Bench (figures 2 and 9). Although previous workers have identified different facies of the Basalt of Antelope Flat (Dossett and others, 2012), we use the geochemical and paleomagnetic results to reinterpret some of these facies. Our results suggest that the paleocanyon-filling facies and the pillow-bearing rim facies on Pine Creek Bench are distinct lava flows, unrelated to the eruption of the Basalt of Antelope Flat.

In figures 7 and 9, we compare our geochemical and paleomagnetic analyses to other basalt samples from Antelope Flat and Pine Creek Bench (Anders and others, 1989; Dossett and others, 2012). Our sample is geochemically most similar to basalts sampled at locations 2 and 4 (figure 8). Our site mean direction of the cored dam complex facies is indistinguishable from site results obtained at locations 3 and 4 (figures 8 and 9). We thus conclude that samples collected from locations 1 through 4 are the Basalt of Antelope Flat.

The lavas sampled at locations 5 and 8 (figure 8) are geochemically distinct from the Basalt of Antelope Flat, with lower SiO_2 and MgO, and elevated FeO^T, P_2O_5, and

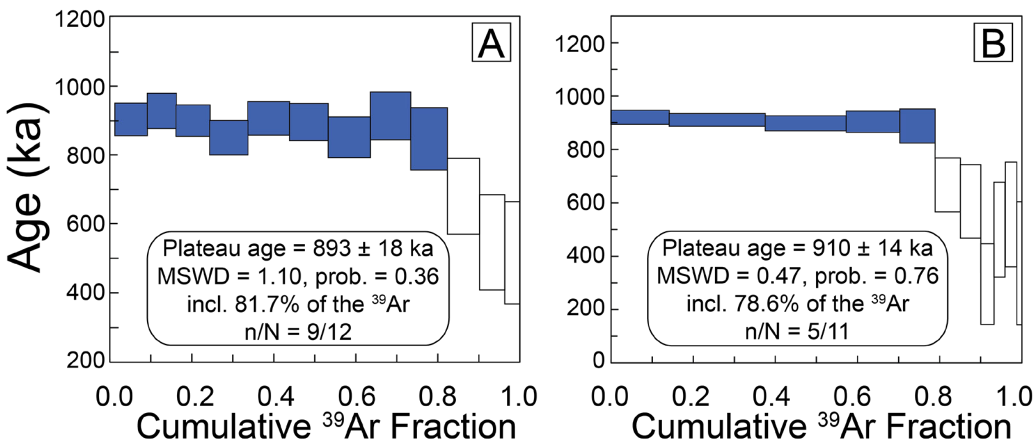

Figure 6. $^{40}Ar/^{39}Ar$ incremental heating analyses of groundmass from Basalt of Antelope Flat (sample 16AF-1). Open boxes are steps excluded from the calculation of the plateau age. MSWD: mean square weighted deviate, prob.: probability, n/N: number of steps included/total number of steps.

TiO_2 (figure 7). These lavas are present at the mouth of Pine Creek Canyon and on the eastern side of the Snake River Canyon, separated from Antelope Flat, which is west of the Snake River (figure 8). Furthermore, their paleomagnetic site mean directions are distinct from the Basalt of Antelope Flat, and each other. These variations lead us to conclude that samples collected from sites 5 through 10 do not represent the Basalt of Antelope Flat. We further conclude from the paleomagnetic results of Anders and others (1989) and Dossett and others (2012) that basalt samples from locations 5 and 6 represent one lava flow that is geochemically similar to, but temporally distinct from, a second lava flow sampled at sites 7 through 10. A possible, and we argue parsimonious, explanation for the distinct site mean directions at locations 5 and 6 compared to locations 7 through 10 is geomagnetic secular variation during the Matuyama Reversal, which could be tested with new radioisotopic dates of these lavas. Alternatively, slip along an unmapped structure between the two location groups could explain the different site mean directions, but our current knowledge of the local geology does not support this interpretation.

Well logs presented by Dossett and others (2012) provide additional evidence for multiple flows. Although they grouped all Quaternary basalts into the Basalt of Antelope Flat and assigned different flow facies, the well logs show significantly thicker lava (about 120 m) on Pine Creek Bench, and thinner basalt (15 to 30 m) along the Snake River Canyon. The thickness of the lavas in Pine Creek Canyon was interpreted as the Basalt of Antelope Flat filling a paleochannel, which allowed for the accumulation of the thick lava (Moore and Embree, 2016). However, geochemical and paleomagnetic evidence suggest that the lava in Pine Creek Canyon is not the Basalt of Antelope Flat. Thus, we conclude that there are at least four distinct basaltic lavas within the Swan Valley graben (figure 8 and table 2):

1. The Basalt of Antelope Flat, with an eruption age of 900 ka, dammed the Snake River and produced the hyaloclastite and associated subaerial lavas. This lava is sampled at locations 1 through 4 and includes samples collected in this work and by Dossett and others (2012).

2. Pine Creek Basalt 1 corresponds to locations 5 and 6 sampled by Dossett and others (2012). These lavas share similar site mean magnetic directions, which are distinct from the other lavas discussed here. These lavas are undated.

3. Pine Creek Basalt 2 corresponds to locations 7 through 10 sampled by Anders and others (1989) and Dossett and others (2012). These lavas share similar site mean magnetic directions, which are distinct from Pine Creek Basalt 1 and the Basalt of Antelope Flat. The lava sampled at location 10 was dated by K/Ar to 1.5 ± 0.8 Ma (Anders and others,

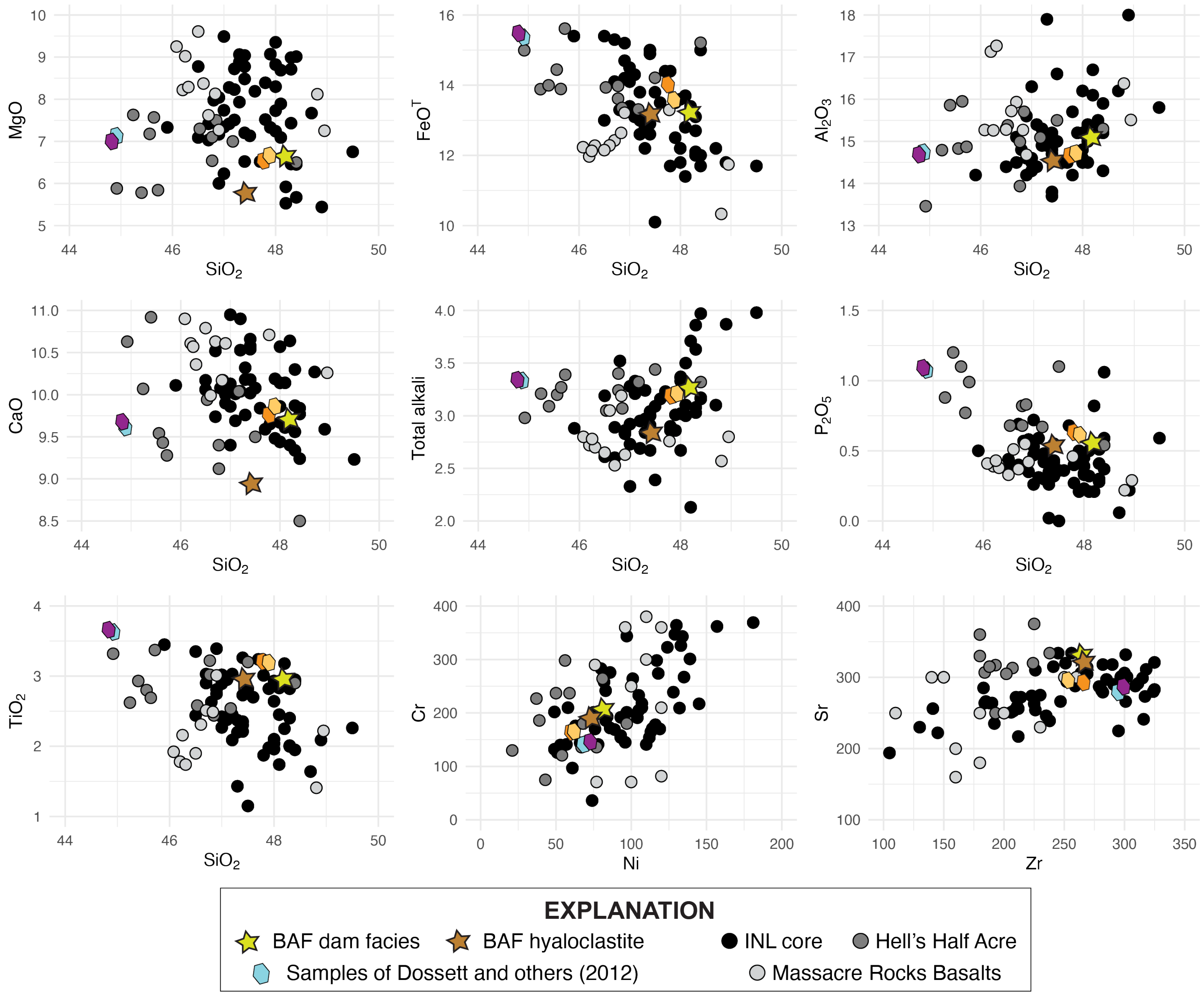

Figure 7. Bivariate plots of selected major element oxides (wt.%) and trace element concentrations (ppm). Data for Basalt of Antelope Flat (BAF) dam facies and hyaloclastite are from this study. Samples from Dossett and others (2012) are the same as those featured in figures 2 and 8. Other Snake River Plain basalt chemistry is from Massacre Rocks (Trimble and others, 1976), Hell's Half Acre (Karlo, 1977), an INL drill core (Shervais and others, 1994), and downloaded via NAVDAT (www.navdat.org). Locations are provided in figure 1.

1989) and was later assigned to the Basalt of Antelope Flat paleocanyon-filling facies (Dossett and others, 2012). Here, we interpret Pine Creek Basalt 2 as distinct from the Basalt of Antelope Flat.

4. Finally, the sample collected at location 11 is a basalt flow that must be older than 2.08 Ma because it underlies the Huckleberry Ridge Tuff. Its composition is characterized by elevated SiO_2 and MgO, and lower total alkalis, P_2O_5, and TiO_2. This basalt has been termed the Basalt of Swan Valley (Dossett and others, 2012) and was dated by K/Ar to 4.0 ± 1.0 Ma (Anders and others, 1989).

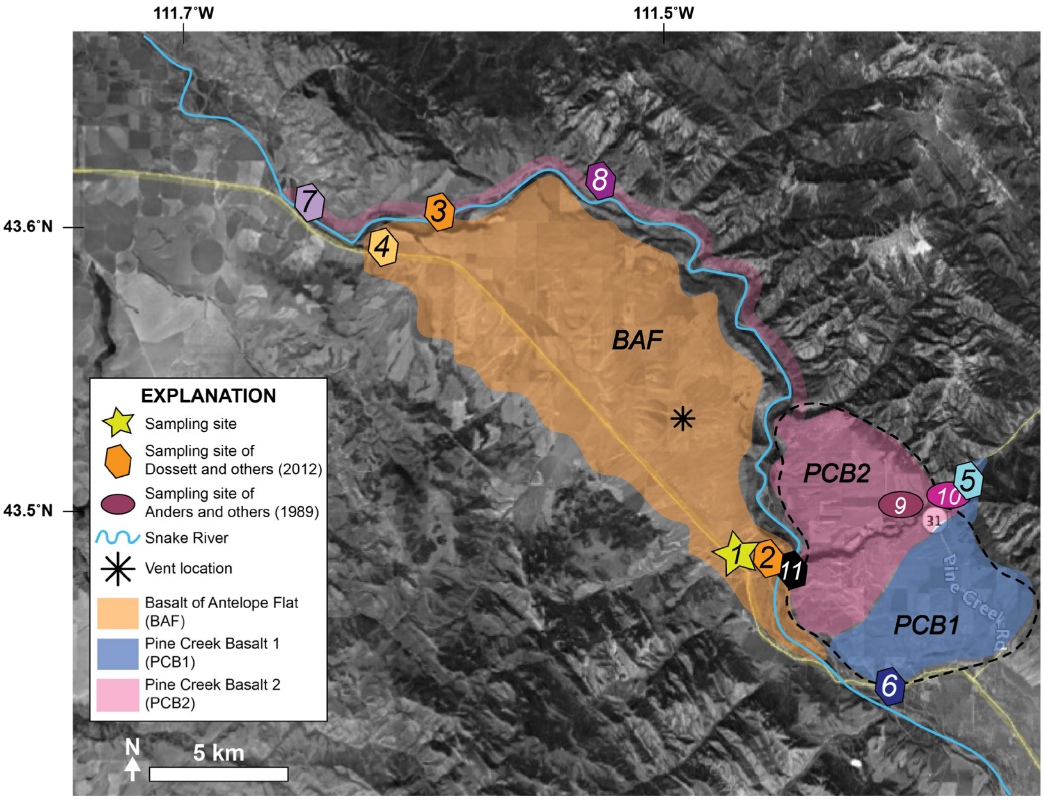

Figure 8. Interpreted distribution of the Basalt of Antelope Flat, Pine Creek Basalt 1, and Pine Creek Basalt 2 based on geochemistry, paleomagnetism, and unit thicknesses in well logs. The Basalt of Antelope Flat has a geochemical and paleomagnetic signature that is distinct from the Pine Creek Basalts. The contact between PCB1 and PCB2 is not defined by geologic mapping.

Paleo-Swan Lake

Calculations of Area, Volume, and the Duration to Fill

The proposed paleo-Swan Lake occupied the area from the lava dam (sampling site 1 in figure 2) southeast through Swan Valley and may have included the area occupied by present-day Palisades Reservoir, thus occupying approximately twice the area of the modern reservoir (Moore and Embree, 2016). Our sample location, which records the transition from a lacustrine to subaerial environment, marks the surface of the paleo-lake at an elevation of about 1707 m. Using the Google Earth measuring tool to define the area of a polygon, we use the 1707-m contour to trace the area of the paleo-lake from the lava dam to the eastern edge of the Palisades Reservoir. Using this method, our estimated area of Swan Lake is 145 km^2. This maximum area (and consequently, the maximum volume calculated below) assumes that the present-day topography is unchanged by erosion or subsidence from the time of eruption of the Basalt of Antelope Flat at about 900 ka. Next, we use the surface elevation of the valley to represent the lake floor (1607 m). Using our estimated area and elevations, we determined that the volume of Swan Lake was about 14.5 km^3. For comparison, this is approximately the volume of Yellowstone Lake in Yellowstone National Park.

To calculate the amount of time required to fill Swan Lake, we used the annual mean of monthly discharge rates of the Snake River from U.S. Geological Survey gauging stations upstream from Palisades Reservoir in two man-made dam-influenced locations: Flagg Ranch, Wyoming and near Moran, Wyoming. The calculated mean discharge at the Flagg Ranch station is 24.8 m^3/s, but is 40.5 m^3/s near Moran (appendix). The duration to fill can be calculated by dividing the volume by the flow rate: we calculate the duration to fill the estimated about 14.5 km^3 with an input of 24.8 m^3/s and 40.5 m^3/s was approximately 12 to 20 years.

This conceptual model assumes that the lava dam was built instantaneously, relative to the time of formation, yet field evidence indicates that the dam formed incrementally: subaerial lavas are interbedded with hyaloclastite, and hyaloclastite deposits are about 60 m thick (Dossett and others, 2010). Our simplified model also assumes that present-day discharge rates along the

Table 2. Sample location coordinates, corresponding location on figure 2, and sample identifiers for geochemical and paleomagnetic analyses. Samples are compiled from this study, Anders and others (1989), and Dossett and others (2012). No coordinates were provided for locations 9 and 10. Sample 16AF-1 was dated in this study; sample PCB3 was dated by the K/Ar method (Anders and others, 1989).

Figure 2 location	Latitude (˚N)	Longitude (˚E)	Geochemistry	Paleomagnetism	Dating
Basalt of Antelope Flat					
1	43.4892	-111.4497	17AF-2, 17AF-3	17AF-2	16AF-1; Ar/Ar
2	43.4867	-111.4341	SR-Post H		
3	43.6014	-111.5777		SRTR11	
4	43.5907	-111.6108	SF-1	SFP1	
4	43.5905	-111.6114		SFP2	
Pine Creek Basalt 1					
5	43.5201	-111.3370	SR-6	10P05	
6	43.4489	-111.3795		10P04	
Pine Creek Basalt 2					
7	43.6025	-111.6439		SRWF11	
8	43.6057	-111.5086	SR-12	10P03	
9				PCB1	
10				PCB3	K/Ar
Pre-Huckleberry Ridge Tuff (>2.08 Ma)					
11	43.4867	-111.4341	SR-Pre H		

Snake River are similar to those at 0.9 Ma, and assumes a constant bottom depth for Swan Lake, rather than using an integrated bottom depth over the length of the lake to account for the slope of the lakeshore and irregularities in the paleotopography of the valley floor. Furthermore, our model assumes that the lava dam was completely sealed and no leakage occurred from the base or sides of the lava dam. If, however, the lava dam leaked, then the input from the Snake River into Swan Lake must have been greater than the leakage from the dam for the water to become deep enough for pillow lavas to form. Pillow lavas are characteristic of the ocean floor, but they are also prevalent in lacustrine systems or shallow marine settings, and they have been documented in other lava-dammed temporary lakes in Idaho (e.g., Malde, 1971; Howard and others, 1982) and in the Grand Canyon, Arizona (e.g., Crow and others, 2015). Hackett and Morgan (1989) note that individual flows of the Basalt of Antelope Flat grade from basal pillow lavas upward to subaerial pahoehoe, which led them to conclude that the water body was only a few meters deep. Thus, it is feasible that pillow lavas could develop in a relatively shallow Swan Lake that formed when the Snake River backed up within the small canyon around the southwest side of Pine Creek Bench into Conant Valley; this would produce the depth needed to generate the observed pillow lavas. No lacustrine sediments, shorelines, Pleistocene tufa, or fossils have been recognized in Swan Valley that would indicate longevity of paleo-Swan Lake. We conclude this suggests that the lake was dammed, filled, and drained relatively quickly.

Water in shallow ponds may also provide sufficient depth for isolated pillow lavas to develop, such as the pillow lavas at Tabernacle Hill, in west-central Utah (Hintz, 2008). There, the existence of pillow lavas interbedded with tufa and the presence of other phreatomagmatic deposits led Hintz (2008) away from the hypothesis of the basalts interacting with Lake Bonneville and

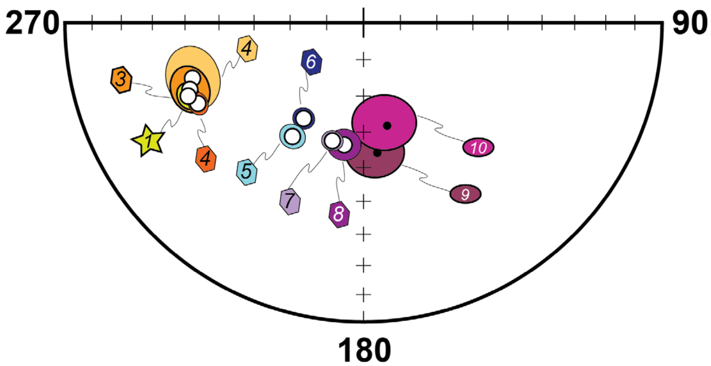

Figure 9. Site mean directions for the Basalt of Antelope Flat sampled in this study (location 1) with paleomagnetic results from Dossett and others (2012) and Anders and others (1989). Note the strong correlation between our results and those from locations 3 and 4. Two additional distinct flows are identified: one flow sampled at locations 5 and 6; and a second flow sampled at locations 7 through 10. Sample identifiers correspond to locations in figure 2 and table 2.

instead toward the interpretation of interaction with pluvial waters. We propose that the interaction of the Basalt of Antelope Flat with the Snake River produced a hyaloclastite dam, which allowed for marsh-like conditions and subsequent formation of pillow lavas in subaerial (rather than subaqueous) waters.

Draining Swan Lake

Moore and Embree (2016) proposed that the lava dam was breached and the water accumulated in Swan Lake incised the present-day canyon that diverts the Snake River to the east of Antelope Flat (figure 8). If Swan Lake drained catastrophically through the modern-day canyon, then we expect to find flood deposits such as scoured bedrock, dry waterfalls, or watermelon boulders. The lack of these deposits, and the absence of shorelines, delta deposits, or sediments and fossils observed as remnants of other Snake River Plain lava-dammed lakes supports our hypothesis of a temporary wetlands or marsh-like environment at the interface between the dam and the Snake River.

In our interpretation, we predict the geometry of the lava dam as shown in figure 10, where the lava dam blocked the area bounded by the hyaloclastite facies deposits on either side of the modern Snake River. As waters rose, the lava dam was breached on the southeastern side, where the Snake River is adjacent to the eastern canyon wall. As the hyaloclastite dam failed from river incision, the Snake River began to carve a path through the Basalt of Antelope Flat and underlying volcanic and sedimentary units. Following dam failure, the Snake River diverted its course to the east, joining with Pine Creek. From this location, the Snake River now cuts a canyon through about 120 m of rock and sediment, comprising the Basalt of Antelope Flat, Pine Creek Basalt 2, the Huckleberry Ridge Tuff, Cenozoic–Quaternary gravels, and is currently incising the 4.0 Ma Basalt of Swan Valley (Anders and others, 1989; Dossett and others, 2012). Optically stimulated luminescence (OSL) dating of a river terrace 5 to 10 m above the modern river suggests that the terrace is about 60 ka (Bufe and others, 2017), and thus that the canyon was largely incised between the eruption of the Basalt of Antelope Flat and 60 ka. Using our new age for the Basalt of Antelope Flat, the 60 ka minimum age for canyon completion and the present-day canyon depth of 120 m, we calculate an average incision rate for the Snake River of 0.014 cm/yr between 900 and 60 ka. We envision that incision was faster following dam failure (due to higher stream power provided by the impounded water, abundance of bed load from dam failure, and an overall wetter climate) and has slowed over time. Our calculated incision rate is consistent with rates previously calculated for this section of the Snake River from 60 ka to present (Bufe and others, 2017). However, it is lower than rates calculated for sections of the Snake River where incision rates may be enhanced by movement along normal faults of the Grand Valley fault system (Tuzlak and others, 2021).

CONCLUSIONS

Snake River Plain volcanism provides geomorphic information about landscape evolution beyond that associated with the migration of North America over the Yellowstone hotspot. The work presented here reports geochemical, geochronological, and paleomagnetic data from the Basalt of Antelope Flat in Swan Valley, Idaho. From these data, we evaluated the eruptive history and interaction with the Snake River within the Swan Valley graben. Paired geochemical and paleomagnetic signa-

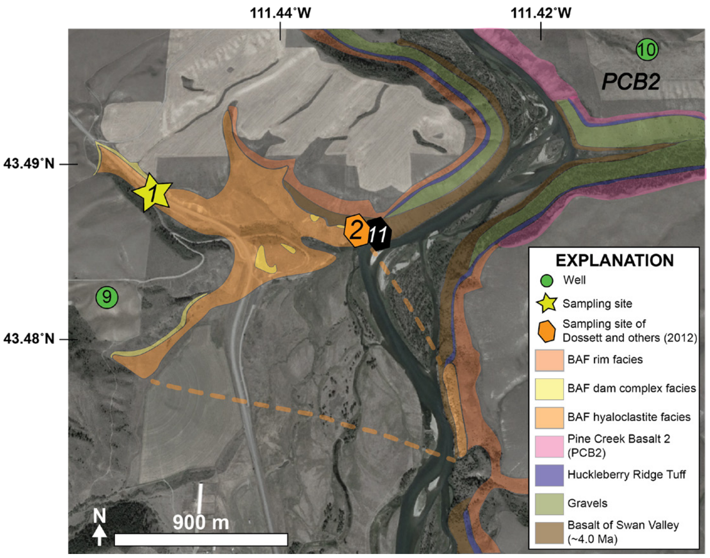

Figure 10. Geology of the Swan Lake dam area. The lava dam would have connected the hyaloclastite facies, as indicated by the dashed lines. Well 9 contains an about 75-m-thick deposit of hyaloclastite; well 10 lacks hyaloclastite but has about 120 m of canyon-filling basalt. Geology and well information from Dossett and others (2012). Geologic contacts, unit thicknesses, and well locations are approximate. The age of the Basalt of Swan Valley is from Anders and others (1989). Imagery from Google Earth, historical image of 2012.

tures of basalts exposed in Swan Valley demonstrate that there are four distinct lavas within Swan Valley: the Basalt of Swan Valley (4.0 Ma), Pine Creek Basalt 1 (undated), Pine Creek Basalt 2 (1.5 Ma), and the Basalt of Antelope Flat (0.9 Ma). The 904 ± 11 ka Basalt of Antelope Flat dammed the South Fork of the Snake River, evidenced by alternating layers of hyaloclastite and dense, subaerial lava at the dam site. Impounded water behind the dam resulted in a temporary marsh-like environment, rather than a long-lived lacustrine environment. When the hyaloclastite dam was breached, the course of the Snake River was diverted eastward, joining Pine Creek and carving the present-day canyon. We calculate an average incision rate through the South Fork of the Snake River canyon of 0.014 cm/yr for the period between 900 and 60 ka, which is consistent with, albeit slightly higher than, rates calculated from 60 ka to present. This rate is less than those calculated for other sections of the Snake River where incision may be influenced by movement along the Grand Valley fault system.

ACKNOWLEDGMENTS

This research was supported by a grant from the National Science Foundation (EAR-1524840). Samples for this work were obtained from the traditional lands of the Shoshone-Bannock people. Many thanks to Dan Moore (Brigham Young University-Idaho) for an introduction to the Basalt of Antelope Flat and Swan Lake story during the 2016 Tobacco Root Geological Society field conference, providing sample 16AF-1, and for continued conversations over the last several years. We thank Doug Sprinkel (Azteca Geosolutions) for editorial handling and Glenn Thackray (Idaho State University) and Joel Pederson (Utah State University) for their insightful reviews.

REFERENCES

Anders, M.H., Geissman, J.W., Piety, L.A., and Sullivan, J.T., 1989, Parabolic distribution of circumeastern Snake River Plain seismicity and latest Quaternary faulting—migratory pattern and association with the Yellowstone hotspot: Journal of Geophysical Research, v. 94, p. 1589, doi: 10.1029/JB094iB02p01589.

Armstrong, R. L., Leeman, W. P., and Malde, H. E., 1975, K-Ar dating, Quaternary and Neogene volcanic rocks of the Snake River Plain, Idaho: American Journal of Science, v. 275, p. 225–251.

Bindeman, I.N., Watts, K.E., Schmitt, A.K., Morgan, L.A., and Shanks, P.W.C., 2007, Voluminous low $\delta^{18}O$ magmas in the late Miocene Heise volcanic field, Idaho—implications for the fate of Yellowstone hotspot calderas: Geology, v. 35, p. 1019, doi: 10.1130/G24141A.1.

Bufe, A., Pederson, J., and Tuzlak, D., 2017, Geomorphic evidence for Quaternary tectonics on the southern flank of the Yellowstone hotspots from terraces and stream profiles along the Hoback and Snake River: EGU General Assembly, v. 19, EGU2017-15867.

Camp, V.E., 1995, Mid-Miocene propagation of the Yellowstone mantle plume head beneath the Columbia River Basalt source region: Geology, v. 23, p. 435–438.

Christiansen, R.L., 1982, Late Cenozoic volcanism of the Island Park area, eastern Idaho *in* Bonnichsen, B., and Breckenridge, R.M., editors, Cenozoic geology of Idaho: Idaho Bureau of Mines and Geology Bulletin 26, p. 345–368.

Christiansen, R.L., 2001, The Quaternary and Pliocene Yellowstone Plateau volcanic field of Wyoming, Idaho, and Montana: U.S. Geological Survey Professional Paper 729-G, 120 p.

Christiansen, R.L., Blank, J., and Richard, H., 1972, Volcanic stratigraphy of the Quaternary rhyolite plateau in Yellowstone National Park: U.S. Geological Survey Professional Paper 729-B, 17 p.

Creighton, D.N., 1987, Menan Buttes, southeastern Idaho, *in* Beus, S.S., editor, Centennial field guide volume 2: Geological Society of America, Rocky Mountain Section, p. 109–111.

Crow, R.S., Karlstrom, K.E., McIntosh, W., Peters, L., Crossey, L., and Eyster, A., 2015, A new model for Quaternary lava dams in Grand Canyon based on $^{40}Ar/^{39}Ar$ dating, basalt geochemistry, and field mapping: Geosphere, v. 11, no. 5, p. 1305–1342, doi: 10.1130/ges01128.1.

Dossett, T.S., Reed, T.H., McIlrath, S.L., Moore, D.K., and Embree, G.F., 2012, Geologic map of the South Fork of the Snake River between Swan Valley and Ririe, Idaho: Idaho Geological Survey, scale 1:24,000.

Fouch, M. J., 2012, The Yellowstone hotspot—plume or not?: Geology, v. 40, p. 479–480.

Greeley, R., 1982, The style of basaltic volcanism in the eastern Snake River Plain, Idaho, *in* Bonnichsen, B., and Breckenridge, R.M., editors, Cenozoic geology of Idaho. Idaho Bureau of Mines and Geology Bulletin 26, p. 407–421.

Hamilton, W., 1965, Geology and petrogenesis of the Island Park Caldera of rhyolite and basalt, eastern Idaho: U.S. Geological Survey Professional Paper 504-C, p. C1–C37.

Hintz, A.R., 2008, Physical volcanology and hazard analysis of a young monogenetic volcanic field: Black Rock desert, Utah: Tampa, University of South Florida, M.S. thesis, 142 p.

Howard, K.A., Shervais, J.W., and McKee, E.H., 1982, Canyon-filling lavas and lava dams on the Boise River, Idaho, and their significance for evaluating downcutting during the last two million years, *in* Bonnichsen, B., and Breckenridge, R.M., editors, Cenozoic geology of Idaho: Idaho Bureau of Mines and Geology, v. 26, p. 629–641.

Hughes, S.S., Wetmore, P.H., and Casper, J.L., 2002, Evolution of Quaternary tholeiitic basalt eruptive centers on the eastern Snake River Plain, Idaho, *in* Bonnichsen, B., White, C.M., and McCurry, M., editors, Tectonic and magmatic evolution of the Snake River Plain volcanic province: Idaho Geological Survey Bulletin 30, p. 363-385.

Humphreys, E.D., Dueker, K.G., Schutt, D.L., and Smith, R.B., 2000, Beneath Yellowstone—evaluating plume and non-plume models using teleseismic images of the upper mantle: GSA Today, v. 10, p. 1–7.

James, D.E., Fouch, M.J., Carlson, R.W., and Roth, J.B., 2011, Slab fragmentation, edge flow and the origin of the Yellowstone hotspot track: Earth and Planetary Science Letters, v. 311, p. 124–135, doi:10.1016/j.epsl.2011.09.007.

Jicha, B.R., Singer, B.S., and Sobol, P., 2016, Re-evaluation of the ages of $^{40}Ar/^{39}Ar$ sanidine standards and supereruptions in the Western U.S. using a Noblesse multi-collector mass spectrometer: Chemical Geology, v. 431, p. 54–66.

Karlo, F.M., 1977, The geology and Bouguer gravity of the Hell's Half Acre area and their relation to volcano-tectonic processes within the Snake River Plain rift zone, Idaho: Buffalo, State University of New York, Ph.D. dissertation, 152 p.

Kirschvink, J.L., 1980, The least-squares line and plane and the analysis of palaeomagnetic data: Geophysical Journal International, v. 62, p. 699–718.

Kuntz, M.A., Spiker, E.C., Rubin, M., Champion, D.E., and Lefebvre, R.H., 1986, Radiocarbon studies of Latest Pleistocene and Holocene lava flows of the Snake River Plain, Idaho—data, lessons, interpretations: Quaternary Research, v. 25, p. 163–176.

Lamb, M.P., Mackey, B.H., and Farley, K.A., 2014, Amphitheater-headed canyons formed by megaflooding at Malad Gorge, Idaho: Proceedings of the National Academy of Sciences, v. 111, p. 57–62, doi:10.1073/pnas.1312251111.

Le Bas, M.J., Le Maitre, R.W., Streckeisen, A., Zanettin, B., and IUGS Subcommission on the Systematics of Igneous Rocks, 1986, A chemical classification of volcanic rocks based on the total alkali-silica diagram: Journal of Petrology, v. 27, p. 745–750, doi: 10.1093/petrology/27.3.745.

Leeman, W.P., 1982, Evolved hybrid lavas from the Snake River Plain, Idaho, *in* Bonnichsen, B., and Breckenridge, R.M., editors, Cenozoic geology of Idaho: Idaho Bureau of Mines and Geology Bulletin 26, p. 193–202.

Leeman, W.P., Vitaliano, C.J., and Prinz, M., 1976, Evolved lavas from the Snake River Plain—Craters of the Moon National Monument, Idaho: Contributions to Mineralogy and Petrology, v. 56, p. 35–60.

Malde, H.E., 1971, History of the Snake River Canyon indicated by revised stratigraphy of the Snake River Group near Hagerman and King Hill, Idaho: U.S. Geological Survey Professional Paper 644-F, p. F1–F21.

Malde, H.E., 1982, The Yahoo Clay, a lacustrine unit impounded by the McKinney basalt in the Snake River Canyon near Bliss, Idaho, *in* Bonnichsen, B., and Breckenridge, R.M., editors, Cenozoic geology of Idaho: Idaho Bureau of Mines and Geology Bulletin 26, p. 617–628.

Matthews, N.E., Vazquez, J.A., and Calvert, A., 2015, Age of the

Lava Creek supereruption and magma chamber assembly at Yellowstone based on $^{40}Ar/^{39}Ar$ and U–Pb dating of sanidine and zircon crystals: Geochemistry, Geophysics, Geosystem, p. 1–21, doi: 10.1002/2015GC005881.

Moore, D.K., and Embree, G.F., 2016, Field guide to the Recent volcanic history of the South Fork area between Swan Valley and Ririe, ID: The Journal of the Tobacco Root Society, v. 45, p. 95–100.

Obradovich, J.D., 1992, Geochronology of the Late Cenozoic volcanism of Yellowstone National Park and adjoining areas, Wyoming and Idaho: U.S. Geological Survey Open-File Report 92-408, p. 1–45.

Pierce, K.L., and Morgan, L.A., 1992, The track of the Yellowstone hot spot—volcanism, faulting, and uplift, *in* Link, P.K., Kuntz, M.A., and Platt, L.B., editors, Regional geology of eastern Idaho and western Wyoming: Geological Society of America Memoir 179, p. 1–54.

Rivera, T.A., Darata, R., Lippert, P.C., Jicha, B.R., and Schmitz, M.D., 2017, The duration of a Yellowstone super-eruption cycle and implications for the age of the Olduvai subchron: Earth and Planetary Science Letters, v. 479, p. 377–386, doi: 10.1016/j.epsl.2017.08.027.

Rivera, T.A., Schmitz, M.D., Crowley, J.L., and Storey, M., 2014, Rapid magma evolution constrained by zircon petrochronology and $^{40}Ar/^{39}Ar$ sanidine ages for the Huckleberry Ridge Tuff, Yellowstone, USA: Geology, v. 42, p. 643–646, doi: 10.1130/G35808.1.

Rivera, T.A., Schmitz, M.D., Jicha, B.R., and Crowley, J.L., 2016, Zircon petrochronology and $^{40}Ar/^{39}Ar$ sanidine dates for the Mesa Falls Tuff—crystal-scale records of magmatic evolution and the short lifespan of a large Yellowstone magma chamber: Journal of Petrology, v. 57, p. 1677–1704, doi: 10.1093/petrology/egw053.

Rivera, T.A., Storey, M., Schmitz, M.D., and Crowley, J.L., 2013, Age intercalibration of $^{40}Ar/^{39}Ar$ sanidine and chemically distinct U/Pb zircon populations from the Alder Creek Rhyolite Quaternary geochronology standard: Chemical Geology, v. 345, p. 87–98.

Scott, W.E., Pierce, K.L., Bradbury, J.P., Forester, R.M., 1982, Revised Quaternary stratigraphy and chronology in the American Falls area, southeastern Idaho, *in* Bonnichsen, B., and Breckenridge, R.M., editors, Cenozoic geology of Idaho: Idaho Bureau of Mines and Geology Bulletin 26, p. 581–595.

Shamloo, H.I., and Till, C.B., 2019, Decadal transition from quiescence to supereruption—petrologic investigation of the Lava Creek Tuff, Yellowstone Caldera, WY: Contributions to Mineralogy and Petrology, v. 174, p. 1–18, doi: 10.1007/s00410-019-1570-x.

Shamloo, H.I., Till, C.B., and Hervig, R.L., 2021, Multi-mode magnesium diffusion in sanidine—applications for geospeedometry in magmatic systems: Geochimica et Cosmochimica Acta, v. 298, p. 55–69.

Shervais, J., Vetter, S., and Hackett, W.R., 1994, Chemical stratigraphy of basalt in coreholes NRP-E and WO-2, Idaho National Engineering Laboratory, Idaho—implications for plume dynamics in the Snake River Plain: Proceedings of the 7th International Symposium on the Observation of the Continental Crust Through Drilling.

Shervais, J.W., and Hanan, B.B., 2008, Lithospheric topography, tilted plumes, and the track of the Snake River-Yellowstone hot spot: Tectonics, v. 27, no. 5, p. 1–17, doi: 10.1029/2007TC002181.

Smith, R.B., and Braile, L.W., 1994, The Yellowstone hotspot: Journal of Volcanology and Geothermal Research, v. 61, p. 121–187.

Stelten, M.E., Cooper, K.M., Vazquez, J.A., Calvert, A.T., and Glessner, J.J.G., 2015, Mechanisms and timescales of generating eruptible rhyolitic magmas at Yellowstone Caldera from zircon and sanidine geochronology and geochemistry: Journal of Petrology, v. 56, p. 1607–1642.

Trimble, D.E., and Carr, W.J., 1976, Geology of the Rockland and Arbon quadrangles, Power County, Idaho: U.S. Geological Survey Bulletin, Report B 1399, 104 p.

Troch, J., Ellis, B.S., Mark, D.F., Bindeman, I.N., Kent, A.J.R., Guillong, M., and Bachmann, O., 2017, Rhyolite generation prior to a Yellowstone supereruption—insights from the Island Park–Mount Jackson rhyolite series: Journal of Petrology. v. 58, p. 29–52.

Tuzlak, D., Pederson, J.L., Bufe, A., and Rittenour, T., 2021, Patterns of incision and deformation on the southern flank of the Yellowstone hotspot from terraces and topography: Geological Society of America Bulletin, v. 134, no. 5-6 p. 1–15, doi: 10.1130/B35923.1.